Int. J. Environ. Res. Public Health **2015**, *12*, 14626-14639; doi:10.3390/ijerph121114626

OPEN ACCESS

International Journal of
Environmental Research and Public Health
ISSN 1660-4601
www.mdpi.com/journal/ijerph

Article

Characterization of La/Fe/TiO_2 and Its Photocatalytic Performance in Ammonia Nitrogen Wastewater

Xianping Luo [1,2,3,4,*], Chunfei Chen [1,3], Jing Yang [1,3], Junyu Wang [1,3], Qun Yan [1,3], Huquan Shi [1] and Chunying Wang [1,2,3]

[1] School of Resources and Environmental Engineering, Jiangxi University of Science and Technology, Ganzhou 341000, China; E-Mails: ccfjxnc@126.com (C.C.); 18270733906@163.com (J.Y.); Wangjunyu1026@163.com (J.W.); yanqun8219893@163.com (Q.Y.); 13177767724@163.com (H.S.); cywang@jxust.edu.cn (C.W.)
[2] Western Mining Co., Ltd., Xining 81006, China
[3] Jiangxi Key Laboratory of Mining & Metallurgy Environmental Pollution Control, Jiangxi University of Science and Technology, Ganzhou 341000, China
[4] Faculty of Engineering, University of Alberta, Edmonton, AB T6G2V4, Canada

* Author to whom correspondence should be addressed; E-Mail: lxp9491@163.com; Tel.: +86-079-7831-2706.

Academic Editor: Miklas Scholz

Received: 3 August 2015 / Accepted: 12 November 2015 / Published: 17 November 2015

Abstract: La/Fe/TiO_2 composite photocatalysts were synthesized by Sol-Gel method and well characterized by powder X-ray diffraction (XRD), scanning electron microscopy (SEM), nitrogen-physical adsorption, and UV-Vis diffuse reflectance spectra (UV-Vis DRS). It is interesting that the doped catalysts were in anatase phase while the pure TiO_2 was in rutile phase. In addition, the composites possessed better physical chemical properties in photocatalytic activity than pure TiO_2: stronger visible-light-response ability, larger specific surface area, and more regular shape in morphology. The photodegradation results of ammonia nitrogen indicate that: the La/Fe/TiO_2 had higher catalytic activity to ammonia nitrogen waste water compared pure TiO_2 and the other single metal-doped TiO_2. pH 10 and 2 mmol/L H_2O_2 were all beneficial to the removal of ammonia nitrogen by La/Fe/TiO_2. However, the common inorganic ions of Cl^-, NO_3^-, SO_4^{2-}, HCO_3^-/CO_3^{2-}, Na^+, K^+, Ca^{2+} and Mg^{2+} in water all inhibited the degradation of ammonia nitrogen. By balance calculation,

at least 20% of ammonia nitrogen was converted to N_2 during the 64.6% removal efficiency of ammonia nitrogen.

Keywords: characterization; photocatalysis; La/Fe/TiO_2; ammonia nitrogen wastewater

1. Introduction

In recent years, a large amount of ammonia nitrogen wastewater was discharged into the water with the mining of rare earth metals in Gannan area, China. Excessive amounts of ammonia nitrogen in water would cause many harmful effects, and the treatment of ammonia nitrogen wastewater is a concern [1]. The methods of chemical precipitation, blow-off, and adsorption are commonly used for the treatment of ammonia nitrogen wastewater at low concentrations. Chemical precipitation method intends to reduce the water solubility of ammonia nitrogen by the formation of indissoluble salt; blow-off method is typically used NaOH to adjust pH to basic of wastewater and ammonia nitrogen would exist in the form of free ammonia (NH_3). Then, ammonia nitrogen would escape from aqueous solution to the atmosphere, which might be difficult to recover and cause the secondary pollution in atmospheric. Adsorption method is mainly based on the ion exchange of NH_4^+ with other cationic ions, which is a reversible process but the exchange capacity is limited [2–4]. The ideal treatment result is that ammonia nitrogen would totally convert to nitrogen. Marco [5] reported that partial of ammonia nitrogen was oxidized to nitrogen by photocatalytic oxidation technology using TiO_2 as the catalyst.

As one of the most promising technologies of treating pollutants in water, photocatalytic oxidation process has received intense attention in many fields and has been researched widely on the environmental protection, health care, building materials and other industries, especially on the photodegradation of pollutants [6–12]. Compared with other advanced oxidation technologies such as Fenton oxidation and ozone oxidation, catalytic wet oxidation, and electrochemical oxidation, photocatalytic oxidation technology is non-toxic and has good stability [13]. Undoubtedly, among the various semiconductor photocatalytic materials, titanium dioxide (TiO_2) is the typical photocatalyst due to its good chemical and biological stability, low cost, ease of availability, and significantly photocatalytic activity under ultraviolet irradiation [14–17]. However, its application remains limited because of its high electron-hole recombination rate in photocatalytic process; another shortcoming of TiO_2 is that it only absorbs ultraviolet light no longer than 387.5 nm, which only accounts for about 4% of sunlight [18–20]. To resolve these problems, one important way is to extend the photoresponse of TiO_2 into visible regions, which has already been studied [11,21,22]; and another important way is to adulterate some amount of metal or nonmetal elements into TiO_2 to increase the migration efficiency of photogenerated electrons and decrease the recombination rate of electron-hole pairs. There are several reports of the photodegradation of ammonia nitrogen by modified TiO_2 [12,23–26]. TiO_2 doped with Fe could utilize visible light wavelengths and effectively produced hydrogen from the decomposition of aqueous NH_3 while TiO_2 doping with rare earth ions playing the key role in the ammonia photocatalytic decomposition [23,24].

Combined with the advantage of iron and rare earth doped TiO_2, La-Fe-codoped TiO_2 was chosen to prepare and the main objectives of this paper are in four aspects: firstly, to investigate the physics

chemical properties of La-Fe-codoped TiO_2 prepared by Sol-Gel method and characterized by XRD, SEM, EDS, and UV-Vis DRS; secondly, to study the photocatalytic activity of prepared doped TiO_2 to ammonia nitrogen; thirdly, to discuss the effect of reaction solution pH, H_2O_2, and common inorganic ions on the degradation of ammonia nitrogen; finally, to disclose the conversion products of ammonia nitrogen during the photodegradation process.

2. Materials and Methods

2.1. Reagents

Tetrabutyl titanate ($Ti(OC_4H_9)_4$), lanthanum nitrate ($La(NO_3)_3$), ferric nitrate ($Fe(NO_3)_3$) and ammonium chloride (NH_4Cl) were of analytical grade and purchased from National Medicine Group Chemical Reagent Co., Ltd., Shanghai, China. Anhydrous ethanol (CH_3CH_2OH) was purchased from Shanghai Zhan Yun Chemical Co., Ltd., Shang hai, China.

2.2. Modification Methods

The photocatalysts were prepared by Sol-Gel method. The mixture solution of 8.5 mL tetrabutyl titanate dissolved in 20 mL anhydrous ethanol with stirring for 30 min was noted as solution A. Another solution containing 20 mL ethanol, 1.5 mL deionized water, and metal salts ($La(NO_3)_3$ and/or $Fe(NO_3)_3$) in the required stoichiometry was noted as solution B. Solution B was pumped into solution A by half drop (*ca.* 0.05 mL) per second at *ca.* 30 °C. The mixture was hydrolyzed at room temperature for a period of time under vigorous stirring and finally the translucent sol was formed. The gel was prepared by aging the sol for two days at room temperature. The dry gel was gained after drying at 80 °C for 2 h. Finally, the gel was calcined at 500 °C at the heating rate of 2.5 °C/min in the muffle furnace for 2 h and was ground into powders for use.

2.3. Characterization

Powder X-ray diffraction (XRD) data were recorded on a D/Max-3c X-ray diffraction meter at 40 kV and 40 mA for monochromatized Cu $K\alpha$ (λ = 1.5418 Å) radiation. Scanning electron microscopy (SEM) measurements were carried out on S-4800 type of field emission scanning electron microscope with energy dispersive spectrometer (EDS). The BET surface areas of the samples were obtained from the automatic analyzer (JW-004A, Beijing JWGB Sci.&Tech. Co.,Ltd, Beijing, China). UV-Vis diffuse reflectance spectra were achieved using a UV-Vis spectrophotometer (UV-2550, Shimadzu China Co., Ltd., Japan), and the absorption spectra were referenced to $BaSO_4$.

2.4. Photocatalytic Removal Experiments and Analytical Methods

The photocatalytic degradation experiments were carried out in a XPA-7 photochemical reactor (Xujiang Electrical Mechanical Plant, Nanjing, China). The irradiation was provided by a 500 W Mercury lamp (Institute of Electric Light Source, Beijing, China), which mainly radiated 365 nm wavelenght of light and was positioned in the cylindrical quartz cold trap. The system was cooled by circulating water and maintained at room temperature. Before the irradiation, the suspension was

magnetically stirred for 30 min in the dark to ensure adsorption equilibrium of ammonia nitrogen on the catalysts. For all the reactions, the irradiation lasted for 300 min. Approximately 5 mL of reaction solution was taken at given time intervals and centrifuged. The supernatant was analyzed by Nessler's reagent spectrophotometry [27] and the removal efficiency (R) was calculated by Formula (1) as follows:

$$R = (C_0 - C)/C_0 \times 100\% \quad (1)$$

where C_0 is the initial concentration of ammonia nitrogen and C is the concentration at reaction time t (min). In order to study the conversion of ammonia nitrogen, NO_2-N and NO_3-N were also detected by spectrophotometry methods [28,29]. In addition, the effects of H_2O_2 and common ions (Cl^-, HCO_3^-/CO_3^{2-}, NO_3^-, SO_4^{2-}, Na^+, K^+, Ca^{2+}, Mg^{2+}) in natural waters on ammonia nitrogen removal were investigated. Besides, all the experiments were performed at least twice and the mean values were reported.

3. Results and Discussion

3.1. Characterization

3.1.1. XRD

The XRD patterns of P25, pure TiO_2, La/TiO_2 and La/Fe/TiO_2 composites are shown in Figure 1. The major peaks at 2θ values of 25.3°, 37.9°, 48.0°, 53.8°, 54.9°, and 62.5° corresponded to diffractions of the (101), (004), (200), (105), (211), and (204) planes of anatase TiO_2 while the major peaks at 27.5°, 36.1°, 39.2°, 41.3°, 44.1°, 54.4°, 56.7°, 62.8°, 64.1°, 65.6°, 69.1° corresponded to diffractions of the (110), (101), (111), (210), (211), (220), (002), (310), and (112) planes of rutile TiO_2. This showed that the pure TiO_2 prepared existed in the rutile phase while the doped catalysts in the anatase phase whether La/TiO_2 or La/Fe/TiO_2. It is interesting to find that the doped rare earth Lanthanum changed the crystal structure of TiO_2 from rutile to anatase. Compared to P25, the crystallinity of doped TiO_2 decreased as shown in Figure 1. Besides, there are no peaks for the formation of composite metal oxides such as La_2O_3 or Fe_2O_3 in doped TiO_2, which might be ascribed to the fact that the concentration of La-doping and/or Fe-doping was so low and the overlapping of diffraction peaks due to TiO_2, La_2O_3, and/or Fe_2O_3.

3.1.2. UV-Vis DRS

The UV-Vis DRS spectra of P25, TiO_2, La/TiO_2, Fe/TiO_2, and La/Fe/TiO_2 are depicted in Figure 2A. All the doped powders showed a redshift compared to P25 while undoped TiO_2 exhibits an absorption edge to the visible light region due to the rutile phase. Besides, there is an obvious change of light absorption of La/Fe/TiO_2 from ultraviolet to visible light due to the La-Fe-codoping. The redshift phenomenon indicates that the modified TiO_2 broaden the scope of light response as anatase phase. In other words, the visible-light-response catalysts overcome the disadvantage of the broadband gap to a certain extent [30]. In addition, the absorption data were analyzed using the following well-known formula for near-edge optical absorption of semiconductors [31].

$$\alpha = A\,(h\upsilon - E_g)^n/h\upsilon \quad (2)$$

where α is the absorption coefficient, ($h\upsilon$) is the photon energy, A is a constant, E_g is the optical gap, and the value of n is 1/2 for TiO_2 [32]. To estimate the optical band gap, the plot of $(\alpha h\upsilon)^2$ *versus* ($h\upsilon$)

is shown in Figure 2B. The E_g values are 3.22, 2.98, 3.01, 3.18, and 2.68 eV for P25, TiO_2, La/TiO_2, Fe/TiO_2 and La/Fe/TiO_2, which indicates that the doped material did broaden the scope of light response of compared with pure TiO_2 and P25.

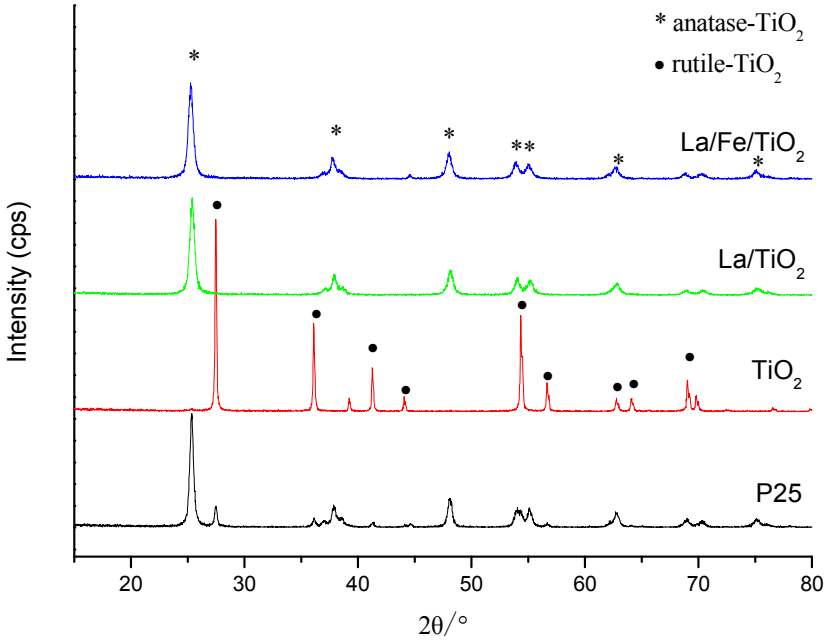

Figure 1. XRD patterns of P25, TiO_2, La/TiO_2 and La/Fe/TiO_2.

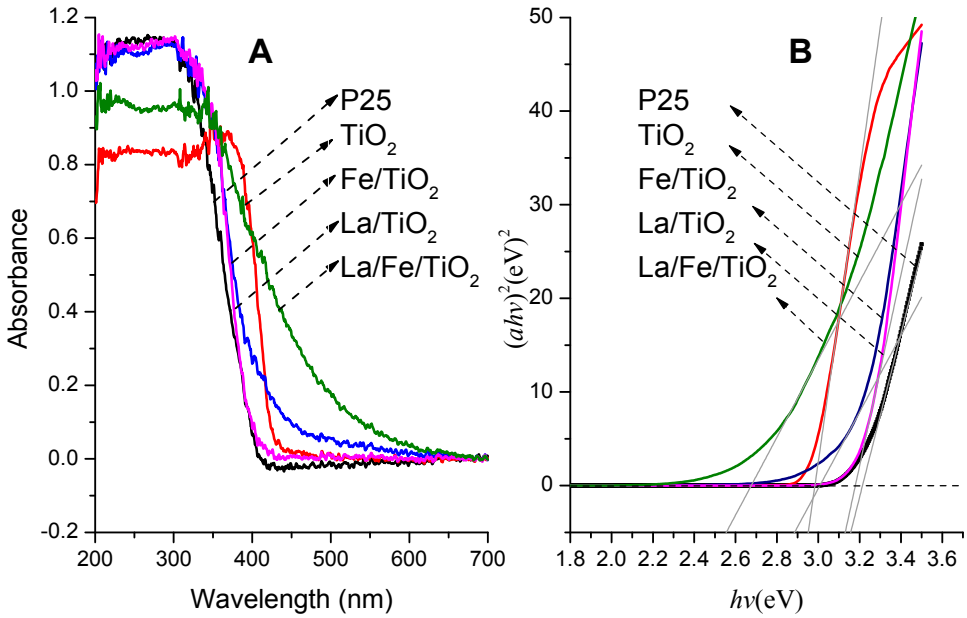

Figure 2. UV-Vis DRS of P25, TiO_2, La/TiO_2 Fe/TiO_2, and La/Fe/TiO_2 ((**A**) Absorbance; (**B**) Plots of $(\alpha h\upsilon)^2$ *versus* ($h\upsilon$) for catalysts).

3.1.3. Surface Morphology Analysis

As seen from Figure 3, pure TiO_2 (Figure 3A) exhibits irregular shape and is agglomerated badly. However, after La and Fe co-doped, the reunion phenomenon is abated and is a relatively flat surface. Compared to Figure 3A and 3B, the more serious reunion phenomenon of pure TiO_2 might be based on

the large amounts of hydroxyl groups on the surface of pure TiO_2 which would result in the strong hydrogen bonding between particles [33].

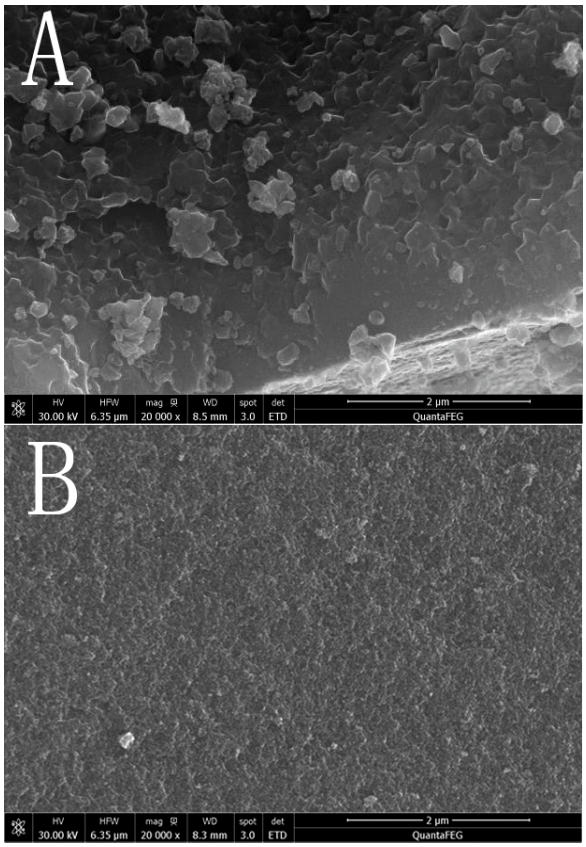

Figure 3. SEM images of TiO_2 (**A**) and La/Fe/TiO_2 (**B**).

Further data for the composition of La/Fe/TiO_2 photocatalysts were obtained by EDS: La accounted for 3.62% while Fe accounted for 0.62%. The result is consistent with the UV-Vis DRS and proves that elements lanthanum and iron were all loaded on the surface of TiO_2.

3.1.4. Specific Surface Area Analysis

The specific surface area of P25, TiO_2, La/TiO_2, and La/Fe/TiO_2 is 48.12, 65.57, 78.36, and 120.74 m^2/g respectively. A significant increase in specific surface area of the doped samples was observed. The increase in specific surface area after doping may be caused by the decrease in the crystallite size of TiO_2, as described in the XRD and SEM part, which is in agreement with Anandan's report that doping of rare earth could increase the surface area of TiO_2 [34].

3.2. Degradation Performance of Ammonia Nitrogen Wastewater

A series of control experiments were designed to investigate the photocatlytic activity of prepared doped composites, and all the experiments were carried out with the same conditions of pH (*ca.* 10), catalyst amount (1 g/L), and 500 W mercury lamp. Figure 4 shows the result. After 5 h, about 15% of ammonia nitrogen was removed by direct photolysis or escaping from the reaction solution by magnetic stirring, while above 50% was removed by photocalytic degradation with catalyst. Furthermore,

the doped catalysts showed higher photocatalytic activity on ammonia nitrogen removal than pure TiO_2 by the analysis of first-order reaction kinetics as shown in Table 1. The best removal efficiency of ammonia nitrogen reached 64.6% with $La/Fe/TiO_2$.

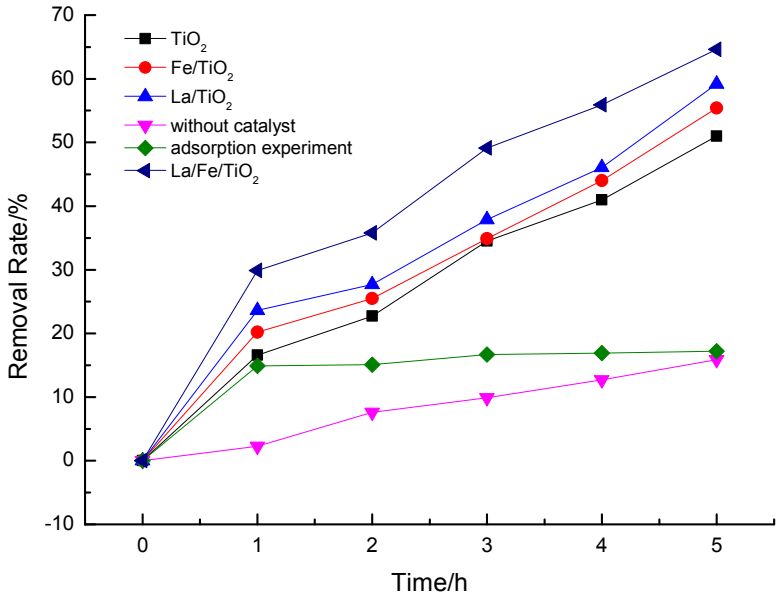

Figure 4. The curves of photocatalysis of NH_4^+-N at different conditions.

Table 1. Reaction kinetics constant of catalysts.

Catalyst	*k*	R^2
TiO_2	0.137	0.990
Fe/TiO_2	0.150	0.988
La/TiO_2	0.163	0.976
$La/Fe/TiO_2$	0.196	0.984

Anandan [34] reported that small particle size, high surface area, high surface roughness, and porous surface of La-doped TiO_2 and the suppression of electron-hole recombination by La^{3+} were the reasons for the high photocatalytic activity of La-doped TiO_2, the characterization result of this study is consistent with their conclusion. Besides, Fe^{3+} is born of the electron capture trap [23]. Under the synergy of La^{3+} and Fe^{3+}, the electron-hole pairs produced from catalyst under irradiation could be effectively separated and the catalytic activity of $La/Fe/TiO_2$ was improved.

3.2.1. Effect of Different pH

The initial pH of the reaction solution might influence the surface charge of $La/Fe/TiO_2$ and the existing form of ammonia nitrogen in water and finally affect the ammonia nitrogen removal efficiency. Firstly, the number of OH^- increases with the pH increases gradually, and more ·OH would be generated induced by $La/Fe/TiO_2$, resulting in promoting the removal rate of ammonia nitrogen. Secondly, there are two forms of ammonia nitrogen in water: $NH_3 \cdot H_2O$ and NH^{4+}. Proportion of $NH_3 \cdot H_2O$ molecules increases as the pH increases in the solution. Thirdly, the space steric hindrance of NH_3 is smaller than that of NH_4^+, which is more conducive to the reaction of NH_3 with ·OH. At last, the pH_{PZC} (point of zero charge) of $La/Fe/TiO_2$ is about 6.4 by analysis of Zeta potential. So, it is difficult for the attraction of

ammonia molecules onto the surface of the catalyst in an acidic condition. All the analysis above demonstrates that ammonia nitrogen was removed rapidly in alkaline environment [35]. However, as shown in Figure 5, it did not favor the catalytic reaction at pH 10.9, which might be due to that excessive OH^- in the solution. The following experiments would be performed at pH *ca.* 10.

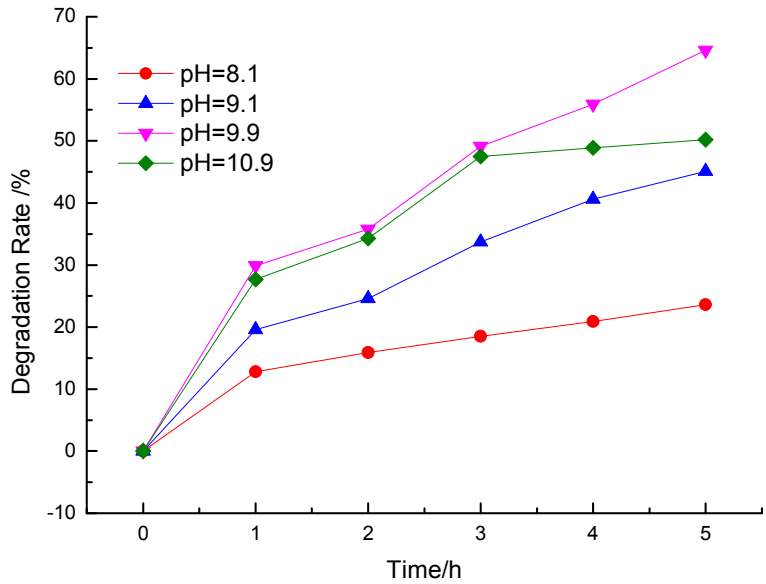

Figure 5. The effect of pH on the degradation of NH_4^+-N with La/Fe/TiO_2.

3.2.2. Effect of H_2O_2

H_2O_2 is usually applied as a stimulator in TiO_2 photocatalysis system to enhance the rate of photocatalytic oxidation [36,37]. In order to investigate the effect of H_2O_2 addition on ammonia nitrogen degradation by La/Fe/TiO_2, experiments were conducted by varying the initial H_2O_2 concentration in the range of 0.01 to 10 mmol/L (0.01, 0.1, 0.5, 2, 10 mmol/L). As shown in Figure 6, addition of H_2O_2 promoted the removal rate of ammonia nitrogen. The removal rate reached 78.3% with H_2O_2 of 2 mmol/L. It is well known that H_2O_2 has strong absorbance in the range of 200–350 nm and could produce ·OH under UV irradiation (Formula (2)). Besides, as a kind of strong oxidizer, H_2O_2 can effectively capture the photoproduction electrons of TiO_2 conduction belt and be converted to ·OH as Formula (3). So, the degradation was accelerated with the addition of H_2O_2.

$$H_2O_2 \xrightarrow{hv} 2 \cdot OH \tag{2}$$

$$H_2O_2 + e^- \rightarrow \cdot OH + HO^- \tag{3}$$

However, excessive H_2O_2 would exhaust the generated $\cdot OH$ in the reaction solution (Formulas (4) and (5)) [38] to reduce the promotion.

$$H_2O_2 + \cdot OH \rightarrow H_2O + \cdot HO_2 \tag{4}$$

$$\cdot HO_2 + \cdot OH \rightarrow H_2O + O_2 \tag{5}$$

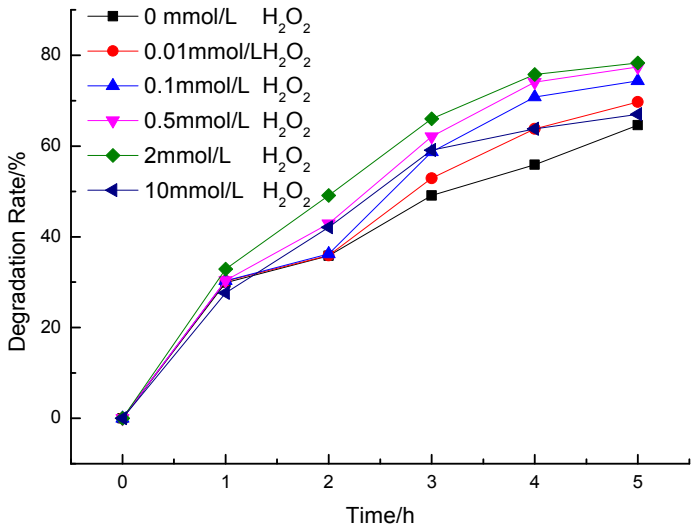

Figure 6. The effect of H_2O_2 on the degradation of NH_4^+-N with La/Fe/TiO_2.

3.2.3. Effects of Inorganic Ions

There are eight common inorganic ions in natural water [39], including Na^+, K^+, Ca^{2+}, Mg^{2+}, Cl^-, SO_4^{2-}, NO_3^-, and HCO_3^-/CO_3^{2-}, and the concentrations are all 0.1 mmol/L. They might affect the removal of pollutants in water. Results of the effects of cations and anions on ammonia nitrogen degradation are shown in Figure 7.

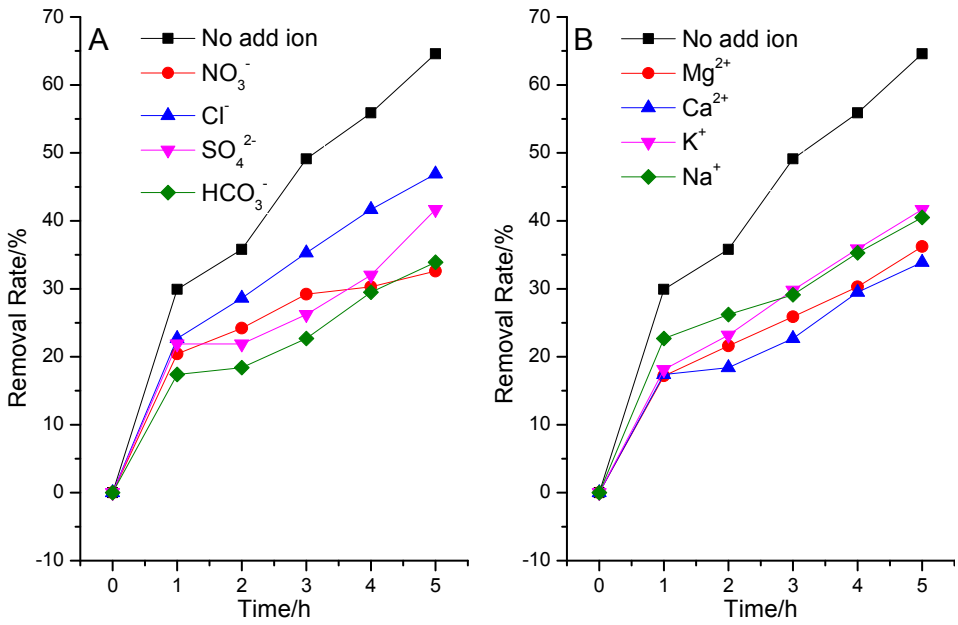

Figure 7. The effect of ions on the degradation of NH^{4+}-N with La/Fe/TiO_2.

As seen from Figure 7, at the same experimental conditions, all kinds of inorganic ions showed an obvious inhibitory effect on ammonia nitrogen removal. Sörensen indicated that NO_3^- acted as an "inner filter" and reduces the UV light intensity in the photoreactor [40]. Thereby, addition of NO_3^- decreased the degradation rate of pollutant in the reaction system. Besides, the inhibited effect increased as the reaction went on. The reason might be that excessive NO_3^- was produced from the conversion of

ammonia nitrogen (the content will be discussed below). It was reported that HCO_3^-/CO_3^{2-} is an effective ·OH scavenger [40]. It can react with ·OH to produce carbonate radicals, which are weak oxidizing reagents that hardly react with other pollutant molecules. Therefore, HCO_3^-/CO_3^{2-} displayed distinct inhibition effect on the degradation of ammonia nitrogen by La/Fe/TiO_2. Cl^- and SO_4^{2-} also could react with ·OH like HCO_3^-/CO_3^{2-}, but the reaction ability was lower than NO_3^-, and the inhibited effect was smaller than HCO_3^-/CO_3^{2-}. Since SO_4^{2-} is double charged, it may display higher inhibition ability than Cl^-.

Na^+, K^+, Ca^{2+}, and Mg^{2+} are all in the highest and stable oxidation state and cannot capture electrons or holes in solution. It is hypothesized that these metal ions would not show significant impacts on the photo degradation of ammonia nitrogen by La/Fe/TiO_2. As shown in Figure 7B, the four metal ions displayed inhibition effects on ammonia nitrogen removal, which could be attributed to the effect of Cl^- ions co-present in the solution. The metal ions were used in their chloride salts. As described above, Cl^- ions might inhibit the photo degradation due to the reaction with ·OH. Since K^+ and Na^+ are in the same elemental main group, they have similar properties. KCl showed similar effect as NaCl. In addition, Ca^{2+} and Mg^{2+} also have similar properties and they ($CaCl_2$ and $MgCl_2$) displayed similar trends. Furthermore, Ca^{2+} and Mg^{2+} displayed higher inhibition effects than NaCl and KCl at the same mole concentrations. This is expected since the concentration of Cl^- in $CaCl_2$ and $MgCl_2$ solutions was twice of that in NaCl and KCl solutions [41]. Besides, Mg^{2+} and Ca^{2+} tend to form precipitation and adhere to the surface of the catalyst to reduce the photocatalytic efficiency in weak alkaline conditions [42].

3.2.4. Analysis of Degradation Products of Ammonia Nitrogen

WuJie [43] mentioned that the process of photodegradation of inorganic nitrogen in water would generate highly reactive ·OH and O_2^- and other reactive oxygen species, which have photocatalytic ability. Inorganic nitrogen ions can induce a series of REDOX reactions, mainly containing NH_4^+ oxidation and NO_3^- reduction (Formulas (6–10)). However, the specific mechanism is still not yet confirmed, and it needs further research.

$$NH_4^+ + 2OH^- \rightarrow NO_2^- + 3H_2 \quad (6)$$

$$2NO_2^- + O_2 \rightarrow 2NO_3^- \quad (7)$$

$$NO_3^- + 2H^+ + 2e_{ab}^- \rightarrow ON_2^- + H_2O \quad (8)$$

$$NO_3^- + 10H^+ + 8e_{ab}^- \rightarrow NH_4^+ + 3H_2O \quad (9)$$

$$2NO_3^- + 12H^+ + 10e_{ab}^- \rightarrow 2N_2 + 3H_2O \quad (10)$$

NO_3-N and NO_2-N were detected as the photocatalytic degradation products of ammonia nitrogen wastewater as the following Figure 8. After 300 min of photocatalytic reaction using La/Fe/TiO_2 as the photocatalyst, the concentration of ammonia nitrogen reached to 34.96 mg/L by the initial concentration of 100.67 mg/L and the conversion rate was 64.6%. During the degradation process, 9.56 mg/L of NO_3-N and 2.07 mg/L of NO_2-N were generated. Considering the escape free ammonia and adsorption part onto the catalyst's surface, it is proposed that at least 20% of ammonia nitrogen was converted to N_2 according to the mass balance of the total nitrogen [44].

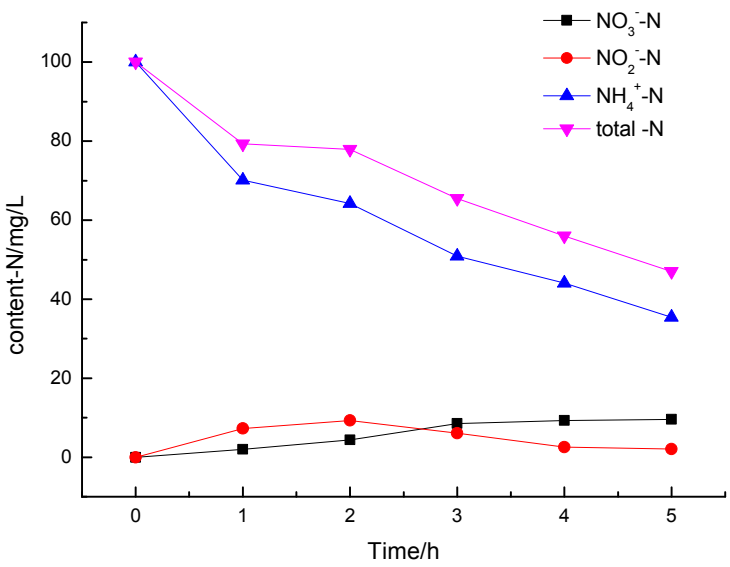

Figure 8. The conversion curves of the NH_4^+-N during the photodegradation process.

4. Conclusions

La-Fe-codoped catalyst demonstrates better physical chemical properties in photocatalytic activity than pure TiO_2: first of all, the doped catalysts were in anatase phase while the pure TiO_2 was in rutile phase; second, the composites possessed strong visible-light-response ability; third, La/Fe/TiO_2 had larger specific surface area and more regular shape in morphology. Furthermore, the doped catalysts indicated higher photocatalytic degradation ability to ammonia nitrogen wastewater: the removal rate of ammonia nitrogen reached to 78.3% at the conditions of pH 9.9, 100.67 mg/L of ammonia nitrogen, 1 g/L of catalyst, and 2 mmol/L of H_2O_2. Besides, the common inorganic ions in water all inhibited the degradation of ammonia nitrogen. At last, it is proposed that there at least 20% of ammonia nitrogen was converted to nitrogen gas during the photodegradation process with 64.6% removal efficiency of ammonia nitrogen.

Acknowledgments

The authors gratefully acknowledge the financial support of "Twelfth five-year" national science and technology support programme (2012 BAC11b07); The ministry of education in the new century excellent talents to support plan (NCET-10-0183); National natural science foundation of China (51408277); "Jiangxi province talent project 555" Talents training plan; Major disciplines in Jiangxi province and technology leaders to develop a target projects (2010 DD01200); Jiangxi province natural science fund project (20122 BAB203027); Jiangxi Students' innovation and entrepreneurship training program (201410407022). Moreover, the authors extends special thanks to the team of Xu Zhenghe professors for their continuous support and help with the experiment of this article.

Author Contributions

Xianping Luo: Presented the original idea for the study. Chunfei Chen, Jing Yang, Junyu Wang, and Huqua Shi: Carried out the experiment, analyzed the data and drafted the manuscript. Qun Yan and

Chunying Wang: Scientific supervisors of all processes including writing. All authors have read and approved the final manuscript.

Conflicts of Interest

The authors declare no conflict of interest.

References

1. Yu, H.; Xu, L.; Wang, P.; Wang, X.; Yu, J. Enhanced photoinduced stability and photocatalytic activity of AgBr photocatalyst by surface modification of Fe(III) cocatalyst. *Appl. Catal. B Environ.* **2014**, *144*, 75–82.
2. Alshameri, A.; Ibrahim, A.; Assabri, A.M.; Lei, X.; Wang, H.; Yan, C. The investigation into the ammonium removal performance of Yemeni natural zeolite: Modification, ion exchange mechanism, and thermodynamics. *Powder Technol.* **2014**, *258*, 20–31.
3. Qu, D.; Sun, D.; Wang, H.; Yun, Y. Experimental study of ammonia removal from water by modified direct contact membrane distillation. *Desalination* **2013**, *326*, 135–140.
4. Iwata, R.; Yamauchi, T.; Hirota, Y.; Aoki, M.; Shimazu, T. Reaction kinetics of ammonia absorption/desorption of metal salts. *Appl. Therm. Eng.* **2014**, *72*, 244–249.
5. Altomare, M.; Selli, E. Effects of metal nanoparticles deposition on the photocatalytic oxidation of ammonia in TiO_2 aqueous suspensions. *Catal. Today* **2013**, *209*, 127–133.
6. Seyedjamali, H.; Pirisedigh, A. *In situ* sol-gel fabrication of new poly(amide-ether-imide)/titania (TiO_2) nanocomposite thin films containing L-leucine moieties. *Colloid Polym. Sci.* **2011**, *289*, 15–20.
7. Gomez, S.; Marchena, C.L.; Pizzio, L.; Pierella, L. Preparation and characterization of TiO_2/HZSM-11 zeolite for photodegradation of dichlorvos in aqueous solution. *J. Hazard. Mater.* **2013**, *258–259*, 19–26.
8. Četojević-Simin, D.D.; Armaković, S.J.; Šojić, D.V.; Abramović, B.F. Toxicity assessment of metoprolol and its photodegradation mixtures obtained by using different type of TiO_2 catalysts in the mammalian cell lines. *Sci. Total Environ.* **2013**, *463–464*, 968–974.
9. Daels, N.; Radoicic, M.; Radetic, M.; van Hulle, S.W.H.; de Clerck, K. Functionalisation of electrospun polymer nanofibre membranes with TiO_2 nanoparticles in view of dissolved organic matter photodegradation. *Sep. Purif. Technol.* **2014**, *133*, 282–290.
10. Zhou, W.; Pan, K.; Qu, Y.; Sun, F.; Tian, C.; Ren, Z.; Tian, G.; Fu, H. Photodegradation of organic contamination in wastewaters by bonding TiO_2/single-walled carbon nanotube composites with enhanced photocatalytic activity. *Chemosphere* **2010**, *81*, 555–561.
11. Pelaez, M.; Nolan, N.T.; Pillai, S.C.; Seery, M.K.; Falaras, P.; Kontos, A.G.; Dunlop, P.S.M.; Hamilton, J.W.J.; Byrne, J.A.; O'Shea, K.; *et al.* A review on the visible light active titanium dioxide photocatalysts for environmental applications. *Appl. Catal. B Environ.* **2012**, *125*, 331–349.
12. Sun, D.; Sun, W.; Yang, W.; Li, Q.; Shang, J.K. Efficient photocatalytic removal of aqueous NH_4^+–NH_3 by palladium-modified nitrogen-doped titanium oxide nanoparticles under visible light illumination, even in weak alkaline solutions. *Chem. Eng. J.* **2015**, *264*, 728–734.

13. Glaze, W.H.; Kang, J.-W.; Chapin, D.H. The chemistry of water treatment processes involving ozone, hydrogen peroxide and ultraviolet Radiation. *Ozone Sci. Eng.* **1987**, *9*, 335–352.
14. Ohko, Y.; Ando, I.; Niwa, C. Degradation of bisphenol A in water by TiO_2 photocatalyst. *Environ. Sci. Technol.* **2001**, *35*, 2365–2368.
15. Grabowska, E.; Reszczyńska, J.; Zaleska, A. Mechanism of phenol photodegradation in the presence of pure and modified-TiO_2: A review. *Water Res.* **2012**, *46*, 5453–5471.
16. Ochiai, T.; Fujishima, A. Photoelectrochemical properties of TiO_2 photocatalyst and its applications for environmental purification. *J. Photochem. Photobiol. C Photochem. Rev.* **2012**, *13*, 247–262.
17. Daghrir, R.; Drogui, P.; Robert, D. Modified TiO_2 for environmental photocatalytic applications: A review. *Ind. Eng. Chem. Res.* **2013**, *52*, 3581–3599.
18. Linsebigler, A.L.; Lu, G.; Yates, J.T. Photocatalysis on TiO_2 surfaces: Principles, mechanisms, and selected results. *Chem. Rev.* **1995**, *95*, 735–758.
19. Asahi, R.; Morikawa, T.; Ohwaki, T.; Aoki, K.; Taga, Y. Visible-light photocatalysis in nitrogen-doped titanium oxides. *Science* **2001**, *293*, 269–271.
20. Yu, J.C.; Zhang, L.; Zheng, Z.; Zhao, J. Synthesis and characterization of phosphated mesoporous titanium dioxide with high photocatalytic activity. *Chem. Mater.* **2003**, *15*, 2280–2286.
21. Chen, X.; Liu, L.; Yu, P.Y.; Mao, S.S. Increasing solar absorption for photocatalysis with black hydrogenated Titanium Dioxide nanocrystals. *Science* **2011**, *331*, 746–750.
22. Kumar, S.G.; Devi, L.G. Review on modified TiO_2 photocatalysis under UV/Visible light: Selected results and related mechanisms on interfacial charge carrier transfer dynamics. *J. Phys. Chem. A* **2011**, *115*, 13211–13241.
23. Obata, K.; Kishishita, K.; Okemoto, A.; Taniya, K.; Ichihashi, Y.; Nishiyama, S. Photocatalytic Decomposition of NH_3 over TiO_2 Catalysts Doped with Fe. *Appl. Catal. B Environ.* **2014**, *160–161*, 200–203.
24. Reli, M.; Ambrožová, N.; Šihor, M.; Matějová, L.; Čapek, L.; Obalová, L.; Matěj, Z.; Kotarba, A.; Kočí, K. Novel cerium doped titania catalysts for photocatalytic decomposition of ammonia. *Appl. Catal. B Environ.* **2015**, *178*, 108–116.
25. Altomare, M.; Dozzi, M.V.; Chiarello, G.L.; di Paola, A.; Palmisano, L.; Selli, E. High activity of brookite TiO_2 nanoparticles in the photocatalytic abatement of ammonia in water. *Catal. Today* **2015**, *252*, 184–189.
26. Liu, J.; Liu, B.; Ni, Z.; Deng, Y.; Zhong, C.; Hu, W. Improved catalytic performance of Pt/TiO_2 nanotubes electrode for ammonia oxidation under UV-light illumination. *Electrochim. Acta* **2014**, *150*, 146–150.
27. Shavisi, Y.; Sharifnia, S.; Hosseini, S.N.; Khadivi, M.A. Application of TiO_2/perlite photocatalysis for degradation of ammonia in wastewater. *J. Ind. Eng. Chem.* **2014**, *20*, 278–283.
28. Administration, S.E.P. *Water Quality-Determination of Nitrate-Spectrophotometric Method with Phenol Disulfonic Acid*, 1st ed.; China Standard Press: Bejing, China, 1987; p. 4.
29. Administration, S.E.P. *Water Quality-Determination of Nitrogen (Nitrite)-Spectrophotometric Method*, 1st ed.; China Standard Press: Beijing, China, 1987; p. 4.
30. Jing, J.; Zhang, Y.; Li, W.; Yu, W.W. Visible light driven photodegradation of quinoline over TiO_2/graphene oxide nanocomposites. *J. Catal.* **2014**, *316*, 174–181.

31. Ghobadi, N.; Moradian, R. Strong localization of the charge carriers in CdSe nanostructural films. *Int. Nano Lett.* **2013**, *3*, 1–5.
32. Wang, X.H.; Li, J.G.; Kamiyama, H.; Katada, M.; Ohashi, N.; Moriyoshi, Y.; Ishigaki, T. Pyrogenic Iron(III)-doped TiO_2 nanopowders synthesized in RF thermal plasma: Phase formation, defect structure, band gap, and magnetic properties. *J. Am. Chem. Soc.* **2005**, *127*, 10982–10990.
33. Parshetti, G.K.; Doong, R.-A. Dechlorination and photodegradation of trichloroethylene by Fe/TiO_2 nanocomposites in the presence of nickel ions under anoxic conditions. *Appl. Catal. B Environ.* **2010**, *100*, 116–123.
34. Anandan, S.; Ikuma, Y.; Murugesan, V. Highly active rare-earth-metal La-doped photocatalysts: Fabrication, characterization, and their photocatalytic activity. *Int. J. Photoenergy* **2012**, *2012*, doi:10.1155/2012/921412.
35. Xiaodong, W.; Zhichun, S.; Guo, L.; Duan, W.; Ziran, M. Effects of cerium and vanadium on the activity and selectivity of MnO_x-TiO_2 catalyst for low-temperature NH_3-SCR. *J. Rare Earths* **2011**, *29*, 64–68.
36. Poulios, I.; Micropoulou, E.; Panou, R.; Kostopoulou, E. Photooxidation of eosin Y in the presence of semiconducting oxides. *Appl. Catal. B Environ.* **2003**, *41*, 345–355.
37. Dasary, S.S.R.; Saloni, J.; Fletcher, A.; Anjaneyulu, Y.; Yu, H. Photodegradation of Selected PCBs in the Presence of Nano-TiO_2 as Catalyst and H_2O_2 as an Oxidant. *Int. J. Environ. Res. Public Health* **2010**, *7*, 3987–4001.
38. Sörensen, M.; Frimmel, F.H. Photochemical degradation of hydrophilic xenobiotics in the UVH_2O_2 process: Influence of nitrate on the degradation rate of EDTA, 2-amino-1-naphthalenesulfonate, diphenyl-4-sulfonate and 4,4′-diaminostilbene-2,2′-disulfonate. *Water Res.* **1997**, *31*, 2885–2891.
39. Dai, S. *Environmental Chemistry*, 2nd ed.; Higher Education Press: Beijing, China, 2006; p. 147.
40. Kim, D.H.; Anderson, M.A. Solution factors affecting the photocatalytic and photoelectrocatalytic degradation of formic acid using supported TiO_2 thin films. *J. Photochem. Photobiol. A Chem.* **1996**, *94*, 221–229.
41. Wang, C.; Zhu, L.; Wei, M.; Chen, P.; Shan, G. Photolytic reaction mechanism and impacts of coexisting substances on photodegradation of bisphenol A by Bi_2WO_6 in water. *Water Res.* **2012**, *46*, 845–853.
42. Ren, X.; Liu, H.; Zhang, C.; Cheng, T.; Zhang, G.; Wu, F.; Sun, S. Effects of inorganic cations on photocatalytic reduction of chromium (VI) over TiO_2 thin films *Tech. Equip. Environ. Pollut. Control* **2010**, *2*, 288–292.
43. Jie, W.; Guo, C.J. Photocatalysis degradation of inorganic nitrogen in Water. *Sci.-Tech. Inf. Dev. Econ.* **2005**, *15*, 173–175.
44. Lee, J.; Park, H.; Choi, W. Selective photocatalytic oxidation of NH_3 to N_2 on platinized TiO_2 in water. *Environ. Sci. Technol.* **2002**, *36*, 5462–5468.